Investigation in the Ga-rich side of the Mn-Ga system: Synthesis and crystal structure of MnGa4 and MnGa5-x (x ∼ 0.15)

Monique Tillard, Claude Belin

Investigation in the Ga-rich side of the Mn-Ga system: Synthesis and crystal structure of MnGa$_4$ and MnGa$_{5-x}$ (x ~ 0.15)

Monique TILLARD and Claude BELIN

Agrégats, Interfaces, Matériaux pour l'Énergie
Institut Charles Gerhardt, UMR 5253 CNRS UM2, CC1502,
Université de Montpellier 2, Sciences et Techniques du Languedoc,
2 Place Eugène Bataillon, 34095 Montpellier Cédex, FRANCE

CORRESPONDING AUTHOR: Monique TILLARD

Email: mtillard@univ-montp2.fr, phone 33 4 67 14 48 97, fax 33 4 67 14 33 04

Abstract

Crystalline compounds MnGa$_4$ and MnGa$_{5-x}$ were successfully prepared by direct synthesis from the elements. The crystal structure of MnGa$_4$ was solved and refined in the cubic Im$\overline{3}$m space group, a = 5.5941(2) Å, Z = 2. The compound MnGa$_{5-x}$ was found under two variants: MnGa$_{4.96}$, tetragonal, P4/mnc with a = 6.3395(2), c = 10.0275(7) Å and MnGa$_{4.83}$, triclinic, P$\overline{1}$ with a = 6.3047(5), b = 9.9441(9), c = 18.901(2) Å, α = 90.382(7), β = 90.766(6), γ =

90.356(7) °. The latter can be viewed as a superstructure deriving from the tetragonal form by tripling one parameter of the cell. The structures of $MnGa_4$ and $MnGa_{5-x}$ are built on the basis of a three-dimensional packing of $Mn@Ga_8$ units, cubic in $MnGa_4$ and square antiprismatic in $MnGa_{5-x}$. In the latter these units are more or less distorted and capped by an extra gallium atom.

Introduction

Among intermetallic alloys combining manganese and gallium, those formed with addition of nickel have attracted significant attention as magnetic shape memory materials, like the Heusler phase Ni_2MnGa [1-5]. Ferromagnetic metal/semiconductor layered structures MnGa/GaAs or MnGa/GaN have interesting applications in spintronic devices such as light emitting diodes [6-9]. Due to the particular nature of the elements Mn and Ga, both having several allotropic forms with rather complex structures, their combinations are of special interest and a lot of their binary alloys have been cited in literature. A pioneering approach based on thermal analysis and X-ray studies, has unveiled the richness of the Mn-Ga binary system, found to contain not less than ten intermediate phases [10]. The unit cell parameters and space groups have been given for six of these phases: hexagonal ε-Mn_2Ga, tetragonal ζ_1-Mn_2Ga, rhombohedral η-Mn_xGa (x = 1.1 to 1.6), tetragonal Mn_2Ga_5, cubic $MnGa_4$ and orthorhombic $MnGa_6$. A short but informative report, published several years later, described a compound having the same orthorhombic cell as $MnGa_6$ but with a lesser gallium content, it was identified as $MnGa_{5.2}$ [11]. A few additional contributions were inserted in the redrawn phase diagram published several years later in the second edition of Binary alloy phase diagrams [12]. Curiously, at that time, the compound $MnGa_4$ was not mentioned in the diagram. A look at the Pearson Crystal Structure Database reveals that at least thirteen different structures are listed for Mn-Ga binary compounds [13], but some of them are not very well characterized. Actually, most of these structures were determined before 1988 from powdered samples except four of them that were more recently determined from single

crystals: rhombohedral MnGa [14], tetragonal Mn_3Ga_5 [15], monoclinic $Mn_{123}Ga_{137}$ [16] and cubic $MnGa_4$ [17]. **The latter was qualified of incompletely published work whereas the structure of $MnGa_4$ was reported elsewhere in a general study of the Hume-Rothery intermetallic compounds having the $PtHg_4$ structure [18].** Some of the Mn-Ga binary compounds have been described as quasicrystal approximants. This is precisely the case for orthorhombic Mn_3Ga_5 and Mn_5Ga_7, also for Mn_5Ga_6 (with two closely related orthorhombic cells) and MnGa (two orthorhombic and monoclinic related forms), compounds characterized by means of transmission electron microscopy [19]. Such intermetallic compounds were found to display a pseudo ten-fold distribution of strong diffraction spots and are then considered as crystalline approximants of a quasicrystal containing 45-50 at. % Mn. The latter, discovered in the same work, is a decagonal quasicrystal that displays periodicity along the ten-fold axis. Subsequently, a structural model based on HREM studies, was proposed for the crystalline compound Mn_5Ga_7 found to coexist with the decagonal quasicrystal in the $Mn_{42}Ga_{58}$ alloy [20]. The similarity with the Al-Mn system, in which the first quasicrystal was discovered [21], is most probably at the origin of a renewed interest for the Mn-Ga system.

The first aim of this work was to prepare the Ga-richer phase $MnGa_6$ but so far, attempts have not succeeded. Instead has been obtained a phase identified as $MnGa_{5-x}$, $x \sim 0.15$, the preparation and crystal structure of which are reported below, next to the synthesis and the complete structural determination of $MnGa_4$.

Experimental section

The elements Mn (powder, Fluka > 99%) and Ga (Rhone Poulenc, 6N) were used without further purification. Reagents taken in the appropriate proportions were mixed in weld-sealed tantalum tubes protected from oxidation inside evacuated stainless steel jackets. According to the already known phase diagram, appropriate thermal treatments were applied to samples in a classic horizontal tubular furnace. Homogenization of the melts was obtained by a slow and continuous rotation of the tantalum tube on its axis.

The compound $MnGa_4$ was obtained from a melt containing 18 % at. Mn, heated at 700°C for 15 hours and subsequently quenched. Some small crushed pieces displayed crystallinity so that the structure could be determined from single crystal X-ray data. Their EDX analyses were found in very good agreement with the compound formula.

Because the Ga-rich part of the phase diagram is uncertain, several alloys were prepared with compositions ranging from 0-20 at. % Mn, in this domain any excess of gallium would play the role of metallic flux and then be beneficial to a better crystallization. Starting from a mixture containing 14 at. % Mn, heated and homogenized at 380°C and then slowly cooled at the rate of 10°/h, a crystallized product was obtained. **Several crystalline pieces previously checked by X-ray diffraction were analyzed by EDX spectroscopy. With a Ga/Mn ratio of ~4.9, their composition significantly differs from $MnGa_6$ and is rather close to $MnGa_5$.** Structural studies of these crystals (type A) revealed some unusual extinction conditions within the X-ray diffraction data. Hence, modified thermal treatments (higher temperature up to 500°C and different cooling rates) intended to improve the crystallization step were used, but crystals then obtained still displayed the same characteristics.

A Pb-excess was added as a metallic flux to a Mn-Ga mixture containing 14 at. % Mn which was heated to 600°C before cooling. A few crystals were grown on the surface of the Pb ingot, they were picked to be analyzed by EDX spectroscopy and were found Pb-free. Since they display rather different crystallographic features, they were designated as type B crystals. An other alloy was prepared at 10 at. % Mn and heated without flux at 570°C. From the analysis of some crystalline pieces selected from this preparation, it appears that it also contains type B crystals. The EDX analysis of several type B crystals selected from either experiment (with and without flux) and previously checked by X-ray diffraction, gave a gallium-to-manganese ratio of ~4.9 indicating that type B crystals have the same composition as type A crystals.

The most regular-shaped and best diffracting crystals of each type were chosen for X-ray diffraction intensity measurements. For this purpose, crystals were glued at the tip of a polymer fiber and mounted on the Xcalibur CCD (Oxford diffraction) four-circle diffractometer that uses $MoK\alpha$ radiation. Details on the single crystal data collection and structural refinements are given in table 1. The powder X-ray diffraction patterns were

recorded on a Philips analytical X'pert diffractometer (copper tube and hybrid monochromator).

It was reported that the structure of MnGa$_4$ belongs to the PtHg$_4$-type [18]. In the present work, it was refined both from powder pattern and from single crystal data. The powder pattern of MnGa$_4$ was completely indexed using program Jana2006 [22] with a I-centered cubic cell of 5.5942(3) Å. The single crystals, with a cell parameter of 5.5941(2) Å, confirmed the cubic symmetry and the Im$\overline{3}$m space group. **Unit cell parameters are in very good agreement with those previously reported [18]. The 2964 reflections (including symmetry equivalent and redundant) recorded within the complete diffraction sphere (θ from 5.15 to 35.61°) from the single crystal were used to solve and refine the structure with SHELX programs [23, 24].** The data set was corrected for the absorption effects ($\mu = 33.6$ mm^{-1}) using the procedure included in the CrysAlis software [25]. After merging equivalent reflections, the final data set used for the refinement of atomic positions and displacement parameters contains 57 unique reflections observed according to the criterion I > 2σ(I). The refined parameters are given in table 2.

Crystals of MnGa$_{5-x}$ type A might be indexed in a tetragonal cell with parameters a = 6.3, c = 9.9 Å but such indexation would leave unassigned a large number of intermediate reflections occurring at reciprocal lattice axes. Instead, all these extra diffractions are well indexed in the 3 × 3 × 1 tetragonal super-cell of parameters a = 18.9 Å and c = 9.9 Å (figure 1, blue-filled cells). Yet, examination of the reciprocal lattice revealed strange extinctions of the hkl reflections having h ≠ 3n and k ≠ 3n, suggesting the occurrence of twinning. The first structural model found in this tetragonal super-cell considered as untwinned, refined poorly to a R factor of 30 %. At this stage, a thorough interpretation of the reciprocal lattice was necessary. Actually, this puzzling diffraction figure results from the twinning of an orthorhombic crystal having two unit cell parameters in the b/a special ratio of 3. By a 4-fold rotation around c-axis, the reciprocal lattices of twin components superimpose and the resulting composite reciprocal lattice then simulates a higher tetragonal symmetry.
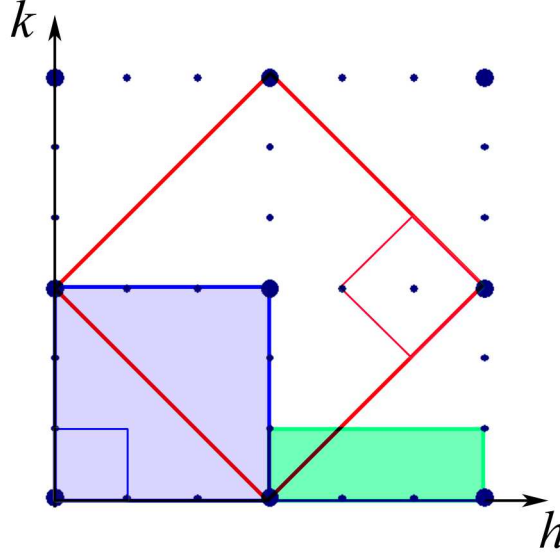
Figure 1: The reciprocal lattice projected along the 9.9Å parameter and the different unit cells mentioned in this paper. The tetragonal cell (a = 6.34, c = 10.03 Å, type B crystals) and its 3 × 3 × 1 super-cell are drawn as large and small blue-filled squares, respectively. The green-filled rectangle refers to the triclinic cell (a = 6.30, b = 18.90, c = 9.94 Å, α = 90.38, β = 90.77, γ = 90.36 °, twin 1 component, type A crystals). The C-centered orthorhombic cell (a = 8.81, b = 8.95, c = 9.94 Å) and its 3 × 3 × 1 super-cell given for $MnGa_6$ in reference [11] are drawn in red.

The overall data could be suitably indexed using two components with an orthorhombic unit cell of parameters a = 6.30, b = 18.89, c = 10.03 Å and the data did not display any centering nor special extinction conditions. However, the angular cell parameters significantly deviate from the 90° angle, this was first attributed to the bad quality of the crystal but it was observed systematically for all the checked crystals. In fact, fine indexation indicates the triclinic cell of parameters a = 6.3047(5), b = 18.9013(15), c = 9.9441(9) Å, α = 90.382(7), b = 90.766(6), γ = 90.356(7) ° for type A crystals (figure 1, green-filled cell). Note that the powder pattern recorded for this alloy can also be properly indexed in the triclinic cell while too many diffraction lines are discarded when indexed using the tetragonal cell.

The reflections recorded within the complete diffraction sphere (θ from 2.96 to 33.00 °) were first corrected for the absorption effects ($\mu = 35.4$ mm^{-1}) in the tetragonal apparent cell of parameters a = 18.9 and c = 9.9 Å. The reflections were divided in two sets: hkl reflections with indices k = 3n which are common to the two twin components, were assigned batch number 2 and hkl reflections with indices k ≠ 3n (twin component 1) batch number 1. The resulting data set of 38305 reflections (8777 unique of which 2942 observed) was then re-indexed in the true triclinic cell and the structure solution was found in the centrosymmetric space group P$\bar{1}$. Structural refinements carried out using SHELXL97 with the HKLF5 instruction and one BASF scale parameter led to a R-factor of 8.47 % and the twin fraction converged to 0.634. The refined parameters are given in table 3 and a selection of interatomic distances in table 4.

Crystals of MnGa$_{5-x}$ type B displayed the perfect tetragonal symmetry with parameters a = 6.3395(2), c = 10.0275(7) Å. Although the existence of close metric relationships with type A crystals might suggest an undetected larger cell for type B, the recorded data for several crystals did not contain any additional diffraction spots regardless of the exposure time. The 9938 recorded reflections (including symmetry equivalent and redundant) within the complete diffraction sphere (θ from 3.80 to 32.04) did not reveal any centering of the cell. Systematic extinctions were observed for 0kl (k+l odd) and hhl (l odd) reflections indicating the possible space groups P4/mnc and P4nc. Data were corrected for absorption effects ($\mu = 35.6$ mm^{-1}) and merged into 373 unique reflections used for the final refinement. Atomic positions and displacement parameters (table 5) were refined to R1 = 3.76 % in the centrosymmetric space group P4/mnc. The main selected interatomic distances are listed in table 6.

Differential thermal analyses (DTA) were performed with a Setaram Labsys analyzer for samples of MnGa$_4$ and MnGa$_{5-x}$. The crystalline powders prepared as described above were inserted in homemade niobium containers which where then sealed under argon atmosphere. Calibration accuracy was verified by measuring the melting points of pure elements (Al, Ag) indicating a maximal standard deviation of 2 °C. For the MnGa$_4$ sample, four endothermal events are observed on the heating curve. The first one, of weak intensity, at about 372 °C was attributed to the peritectic decomposition of MnGa$_{5-x}$ (**present in small quantity as a**

side compound in the sample). The second peak at 397 °C corresponds to the peritectic decomposition of $MnGa_4$. The two following events that occur at higher temperatures, 496 and 535 °C, are characteristic of the peritectic invariants associated with $MnGa_3$ and Mn_2Ga_5 compounds, respectively. The end of melting (liquidus curve) was observed at about 600 °C. On the other hand, the temperature behavior of $MnGa_{5-x}$ samples was also analyzed. The heating curves displayed four endothermal events at 372, 397, 498 and 535 °C, the end of melting could be detected slightly below 600 °C. The first thermal event at 372 °C was attributed to the peritectic decomposition of the compound $MnGa_{5-x}$ while the three following events are related to the successive peritectic decompositions of compounds $MnGa_4$, $MnGa_3$ and Mn_2Ga_5. In the light of these results, the Ga-rich part of the binary diagram was redrawn and a schematic representation is proposed in figure 2. It should be noted that, when heating the $MnGa_{5-x}$ sample, an additional endothermal event of rather small amplitude was observed at a temperature close to 205 °C that could be the sign of the polymorphic phase transition from triclinic to tetragonal $MnGa_{5-x}$.
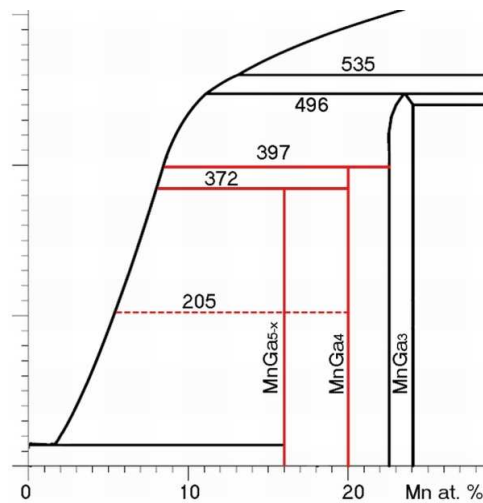

Figure 2: Schematic representation of the Ga-rich side of the Ga-Mn binary diagram.

Calculations were performed at the DFT level with the code CASTEP [26, 27] using the gradient-corrected GGA-PW91 exchange and correlation functional [28]. CASTEP uses plane-wave basis sets to treat valence electrons and pseudo potentials to approximate the potential field of ion cores. Ultra-soft pseudo potentials (USPP) generated for each element according to the Vanderbilt [29] scheme were chosen. Kinetic cut-off energies were set at fine qualities (300 eV) and Monkhorst-Pack uniform grids of automatically generated k-points were used [30].

Results and Discussion

The crystal structure of compound $MnGa_4$ is represented in figure 3. The Ga atoms located at 8c special positions are arranged at the vertices of a cube (Ga-Ga distance of 2.797 Å) centered by Mn atom (2a special position), the Mn-Ga distance is 2.422 Å. The resulting cubic Mn-centered Ga_8 units ($Mn@Ga_8$) are packed within a three-dimensional network by sharing all their corners.

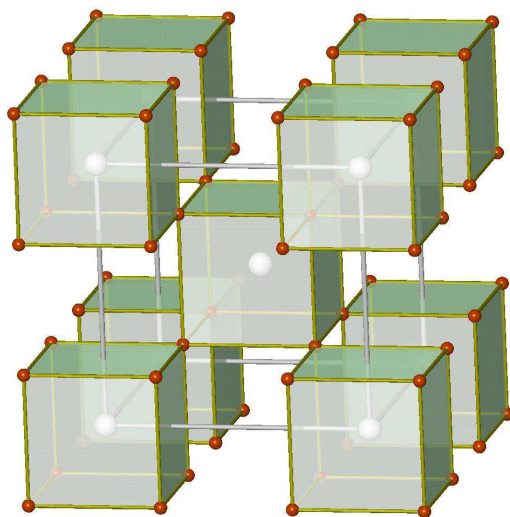Figure 3: The $MnGa_4$ cubic unit cell emphasizing packing of cubic $Mn@Ga_8$ units.

The compound $MnGa_{5-x}$ was found to display either triclinic or tetragonal unit cells. For the triclinic type A and tetragonal type B crystals, structural refinements led to the very close refined compositions $MnGa_{4.83}$ and $MnGa_{4.96}$, respectively. The three-dimensional atomic arrangement mainly proceeds through the packing of distorted square antiprisms of gallium centered by Mn atoms. Though different in geometry from the cubic units in $MnGa_4$, the square antiprismatic units encountered in the $MnGa_{5-x}$ structures can also be formulated $Mn@Ga_8$. Through square face sharing, two $Mn@Ga_8$ antiprisms form a "double drum" unit, which is capped by gallium atoms on its remaining free square faces to finally result into a $Mn_2@Ga_{14}$ oblong unit. The Mn atoms are separated by 3.086 Å in the tetragonal structure of $MnGa_{5-x}$ and the Mn-Mn interatomic distances range from 3.043 to 3.102 Å in the triclinic form. The structure of compound $MnGa_{5-x}$ can be described as a three-dimensional stacking along the c-axis of more or less distorted $Mn_2@Ga_{14}$ oblong units that share basal vertices and are interlinked through waist atoms.
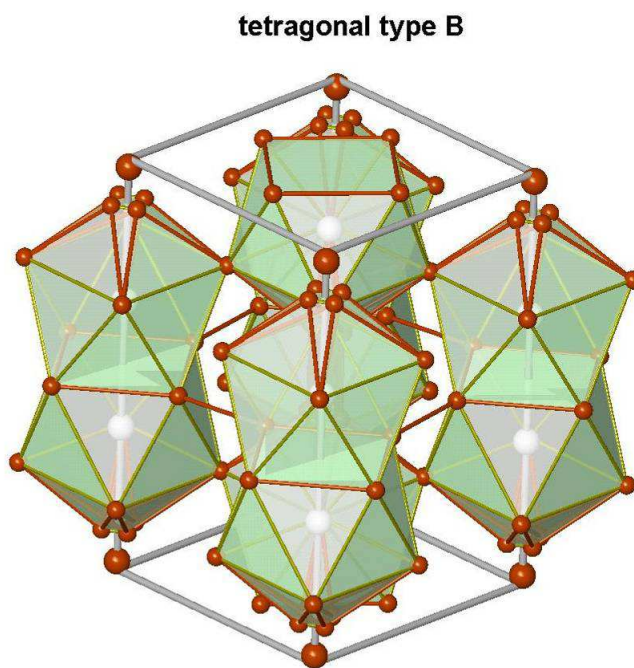

Figure 4: Atomic arrangement in the tetragonal $MnGa_{4.96}$ (type B) unit cell emphasizing the $Mn_2@Ga_{14}$ polyhedra (fused and capped $Mn@Ga_8$ antiprisms).

Beyond symmetry considerations, the atomic arrangement is very close in the two forms of $MnGa_{5-x}$. The main difference between them stems from the occurrence in the tetragonal (type B) structure of some atomic disorder in the capping region (figure 4).

In the course of the structure determination of type B tetragonal crystal, the atoms involved in the $Mn@Ga_8$ square antiprisms were located first and the Fourier synthesis subsequent to the refinement of their atomic parameters revealed two remaining positions for the capping atoms. Actually, these positions are located near the origin of the cell, either on the 4-fold axis at 4e special position (0,0,z) or slightly apart from the axis at a 16i general position and they were assigned to gallium atoms Ga(4) and Ga(5), respectively. Since atoms placed at these sites would be too close, partial site occupation factors had to be taken into account. According to disorder, the 16i general position cannot be filled by more than 25 %, furthermore it should be empty when an atom is present at 4e position. This restrictive condition was tuned by a constrained refinement of Ga(4) and Ga(5) site occupation factors. Even when freely refined, these occupations did not deviate much from their constrained values. The final refined composition is then $MnGa_{4.96(2)}$ for the tetragonal structure.
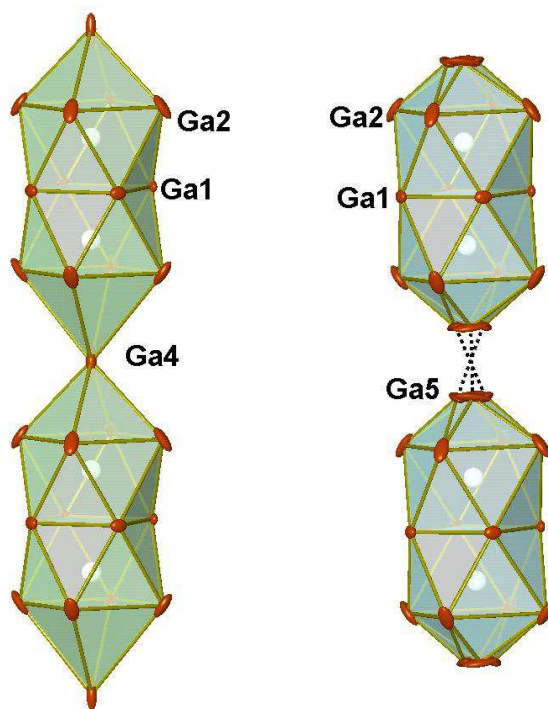
Figure 5: The tetragonal (type B) structure of MnGa$_{5-x}$: apex-sharing or interlinked Mn$_2$@Ga$_{14}$ units depending upon the local disorder.

As expected, expanded ellipsoids featuring the disorder were obtained when the displacement parameters of these atoms were refined anisotropically. Atom Ga(4) displayed an ellipsoid elongation along the c-axis (U$_{33}$ ≈ 5 × U$_{11}$ = 5 × U$_{22}$) while the Ga(5) ellipsoid was found elongated within the ab plane and practically along the b-axis direction (U$_{22}$ ≈ 4 × U$_{11}$ ≈ 11 × U$_{33}$). In summary, the tetragonal structure of MnGa$_{4.96}$ consists of Mn$_2$@Ga$_{14}$ building blocks three dimensionally packed sharing Ga(2) basal vertices and interlinked through Ga(1) waist atoms. Moreover, depending upon the local disorder, these units achieve their coordination through capping, with either Ga(4) apex sharing or Ga(5)-Ga(5) interlinking (figure 5).

Owing to the lower global symmetry, the triclinic structure of MnGa$_{4.83}$ is built of somewhat distorted Mn$_2$@Ga$_{14}$ units that share basal vertices and are interlinked through waist and capping atoms (figure 6).
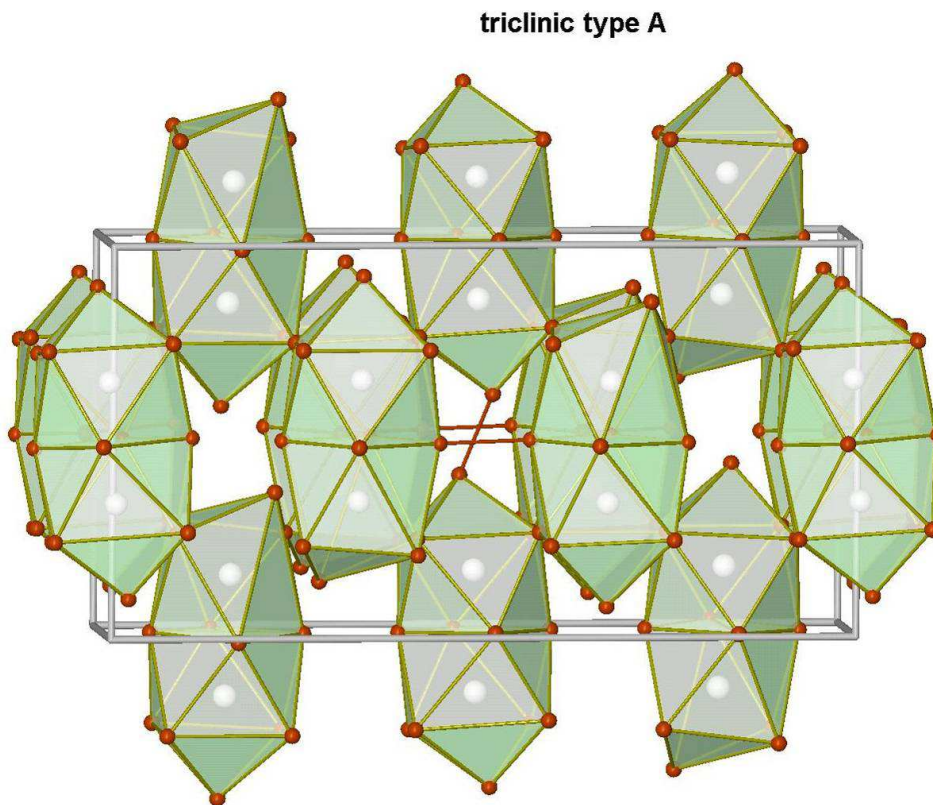
Figure 6: Packing of $Mn_2@Ga_{14}$ polyhedra in the triclinic unit cell of $MnGa_{4.83}$ (type A). Excepted at center of drawing, the interpolyhedral bonding was omitted for clarity

According to the crystallographic results and the very close compositions for the two kinds of crystals studied in this work, we assert that compound $MnGa_{5-x}$ may exist under two polymorphs, depending on subtle variations in the synthesis conditions. The tetragonal structure corresponds to the high temperature form stabilized under specific conditions while the low temperature triclinic structure is obtained by relaxation of packing constraints at the expense of a symmetry loss. This assumption supported by thermal analyses of present work is in agreement with the announced polymorphism for a compound labeled Mn_6Ga_{29} ($MnGa_{4.83}$) which was cited recently in conference abstracts [31, 32]. Furthermore, it has long been known that crystals having high-low temperature transformations possess related symmetries, which allow the main structural framework to be retained. Some symmetry

elements are lost in the low temperature form so that the transformation frequently would give rise to twinning [33].

It is quite usual that gallium and aluminum combine similarly with other elements but, with manganese, they form rather different binary compounds. In addition to the orthorhombic structure of $MnAl_6$, are known those of cubic $MnAl_{12}$ and $MnAl_{4.87}$ as well as those of hexagonal $MnAl_{4.33}$ and $MnAl_{4.11}$ (reported as λ and μ-$MnAl_4$) but no $MnGa_4$ aluminum analogue has been reported. Besides, the existence of a $MnAl_4$ compound having the $PtHg_4$ type was excluded by theoretical investigations [18]. With an Al/Mn ratio of 4.87, very close to the Ga/Mn ratio in $MnGa_{5-x}$, the compound Mn_8Al_{39} yet crystallizes in a very different cubic structure where Mn atoms lie at centers of Al icosahedra (full Al_{12}, atom deficient Al_{11} or Al_{10}) [34]. For the gallium combinations involving transition metals close to manganese such as vanadium, chromium and iron, a look at the reported structures indicates that the gallium richest compounds are V_8Ga_{41}, $CrGa_4$ and $FeGa_3$, respectively. $CrGa_4$ is isostructural to $MnGa_4$ [18] while V_8Ga_{41} contains hybrid (half cube-half icosahedra) $V@Ga_{10}$ polyhedra [35] and $FeGa_3$ is built of Fe-capped distorted $Fe@Ga_8$ square antiprisms [36].

It is now interesting to check present results against those already reported in literature for the Ga-richest binary compounds of manganese. The Ga-rich compound identified as $MnGa_6$ by Meissner et al. was reported to display orthorhombic symmetry with Cccm space group and unit cell parameters a = 8.81, b = 8.95, c = 9.94 Å [10]. Later, Girgis and Schulz obtained a Ga-rich compound whose composition, $MnGa_{5.2}$, was established by chemical analysis [11]. This compound was reported to crystallize as either prismatic or needle-shaped single crystals with the same crystal parameters as $MnGa_6$. Then authors assumed this compound to be a gallium analogue of the compound $MnAl_6$ characterized with Cmcm space group (a = 6.498, b = 7.540, c = 8.858 Å), but the relationship between their cell parameters is not obvious.

On the other hand, it is worth recalling that $MnGa_{5.2}$ diffraction patterns contained some superstructure reflections and special pseudo extinctions [11]. Assuming that a $3 \times 3 \times 1$ superstructure is built from the C-centered orthorhombic cell of parameters a = 8.81, b = 8.95 and c = 9.94 Å (figure 1, red lines), the pseudo-extinctions were attributed by authors to the

non filling (or the only filling) of some special sites in their structure but no further structural characterization has been given. A special attention should be paid to the position of these superstructure reflections which were observed in rows parallel to the [110] and [1$\bar{1}$0] directions.

The reciprocal lattice of MnGa$_{5-x}$ crystals is represented in figure 1, it would be indexed within a C-centered orthorhombic cell of parameters a = 8.81, b = 8.95, c = 9.94 Å (red lines) which is very similar to that previously given for MnGa$_{5.2}$. It is then straightforward to establish a relation between this orthorhombic cell and the unit cells determined in present work for the two MnGa$_{5-x}$ polymorphs: tetragonal (a = 6.34, c = 10.03 Å, blue lines) and triclinic (a = 6.30, b = 18.90, c = 9.94 Å, α = 90.4, β = 90.8, γ = 90.4 °, green lines). Actually, twinning of MnGa$_{5-x}$ triclinic crystals provides additional diffraction spots that occur along the reciprocal axes of the triclinic cell. These axes coincide with the diagonals of the C-centered orthorhombic cell defined just above.

It might be possible that the MnGa$_{5.2}$ crystals obtained by Girgis and Schulz [11] are twinned which would explain the additional spots observed along the diagonals of the orthorhombic cell and the curious extinctions incorrectly attributed to a superstructure. Consequently, it is reasonable to believe that we have obtained the same phase as those previously identified as "MnGa$_{5.2}$" by Girgis or MnGa$_6$ by Meissner. This phase would undergo a polymorphic transformation between two closely related (high and low temperature) crystalline forms and would have a narrow composition domain.

Furthermore, polymorphism is also reported for the compound Mn$_6$Ga$_{29}$ (MnGa$_{4.83}$) [32] which is triclinic below 145 °C, then monoclinic and finally transforms into tetragonal at 210°C [37]. The triclinic and tetragonal cells given for Mn$_6$Ga$_{29}$ are very close to that of triclinic and tetragonal cells of MnGa$_{5-x}$. Although displaying a lower symmetry (P4/m), the tetragonal form of Mn$_6$Ga$_{29}$ looks like the tetragonal P4/mnc MnGa$_{5-x}$ [38]. No sign of phase transformation was detected for MnGa$_{5-x}$ around 145 °C, nevertheless the existence of a monoclinic form, similar to monoclinic Mn$_6$Ga$_{29}$ (a = 6.29, b = 9.97, c = 31.43 Å, β = 90.8 °) claimed to exist in the range 145 – 210 °C [32], cannot be excluded.

Note that we have learnt from a reviewer that Bostrom's dissertation reports work about the Mn-Ga binary system [39]. A Ga-rich compound identified as ω-MnGa$_6$ was obtained either as multi-crystalline fibers or as crystals twinned at the micoscopic level. Its crystal structure, mainly based on capped antiprisms, was described in monoclinic P2 space group (a = 6.295, b = 9.964, c = 18.931 Å, β = 90.88 °). Mn and Ga atoms were not differentiated, several atoms were refined on split positions and temperature factors were not entirely satisfactory so that author believes its structure could be an approximation of a real incommensurate structure. Is is likely that an incorrect symmetry attribution, monoclinic instead of triclinic, would also explain the rather poor quality of this structural determination and very probably, ω-MnGa$_6$ is the same compound as Mn$_6$Ga$_{29}$ and MnGa$_{5-x}$.

In order to analyze bonding in the Mn-Ga binary compounds obtained in present work, geometry optimizations were carried out by varying the cell parameters and the atomic positions. During the optimization, unit cell parameters did not deviate by more than 1.7% from the experimental values. The calculated CASTEP band structures indicate a metallic character for the two compounds MnGa$_4$ and MnGa$_{5-x}$. As can be seen in figure 7 where are represented the partial densities of states (PDOS) calculated for MnGa$_4$ and for the two forms of MnGa$_{5-x}$, atomic contributions in the total density of states (DOS) at Fermi level mostly involve the Ga 4p and Mn 3d states. **This is in very good agreement with FLAPW calculations showing strong covalent bonding between Mn and Ga atoms [18]**. The highest positive values for the overlap populations are calculated for Mn-Ga atomic pairs in the two compounds MnGa$_4$ and MnGa$_{5-x}$. This result indicates that bonding therein is mainly achieved through Mn-Ga bonds.
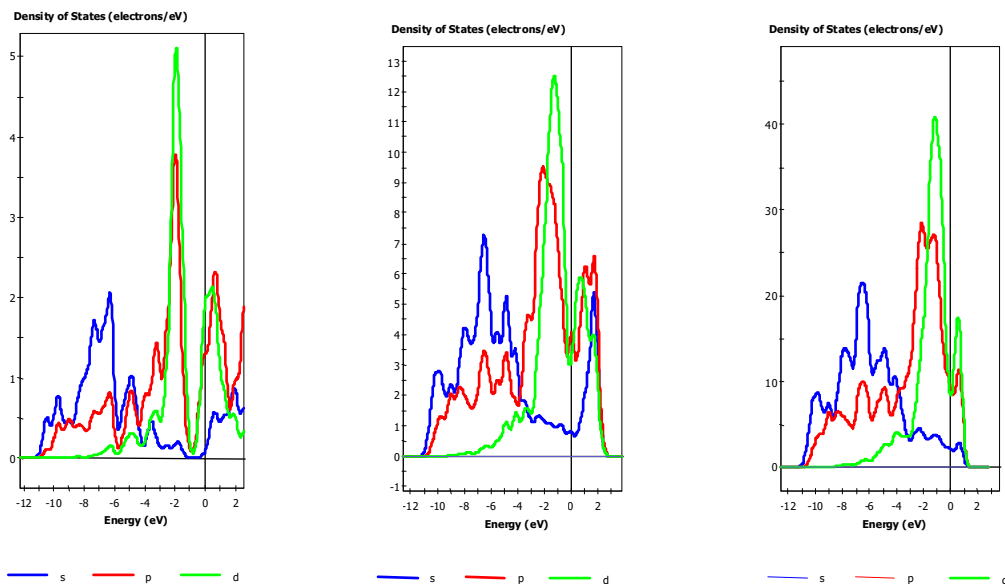
Figure 7: Castep partial densities of states (PDOS) calculated for $MnGa_4$, tetragonal $MnGa_{5-x}$ and triclinic $MnGa_{5-x}$. The total DOS at Fermi level mainly results from gallium 4p and manganese 3d contributions.

For the $MnGa_{5-x}$ structure, high positive values are also associated to the Ga-Ga pairs corresponding to interpolyhedral contacts, sign of a strong interpolyhedral bonding. In the rest of the structure, the overlap populations rather indicate weak or non-bonding (even antibonding) character for the other Ga-Ga interactions. For the two compounds, the atomic Mulliken charges calculated for manganese (between -0.22 and -0.35) and for gallium (from -0.03 to 0.15) are in fairly good agreement with Pearson's electronegativities of the elements (3.7 and 3.2, respectively). Nevertheless, the Mulliken charge and population analyses are known to be basis set dependent and therefore of limited use when calculated with plane-wave DFT methods. A better approach of bonding may be provided by the deformation charge density. This quantity is computed by subtracting the densities of isolated atoms from the total electron density, it shows positive regions indicative of the formation of bonds while negative regions point out electron losses.
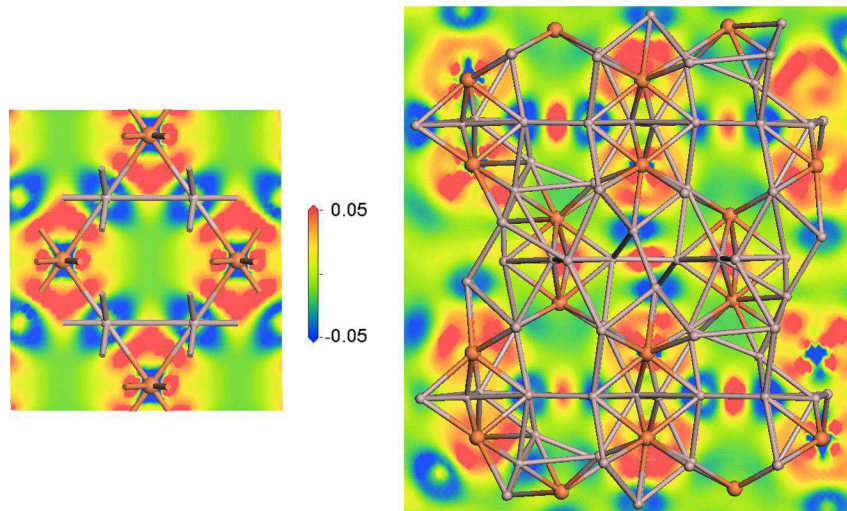
Figure 8: The electron density difference calculated with CASTEP for $MnGa_4$ (left) and triclinic $MnGa_{5-x}$ (right). High densities, indicative of bond formation, are found at Mn-Ga atomic pairs and between the Ga atoms involved in interpolyhedral bonding in $MnGa_{5-x}$

The electron density difference is represented in figure 8 for cubic $MnGa_4$ and triclinic $MnGa_{5-x}$ compounds. The highest positive values of the electron density difference are observed at Mn-Ga atomic pairs and between the gallium atoms involved in interpolyhedral contacts indicative of the covalent character of these bonds. The presence of quite diffuse electron density between all the remaining Ga-Ga atomic pairs accounts for the global metallic character calculated for the compounds. **It worth noting that metallic conductivity of $MnGa_4$ has been experimentally evidenced from resistivity measurements [18].**

5. Conclusion

The structural determinations of $MnGa_4$ and $MnGa_{5-x}$ bring new insights in the knowledge of the gallium rich part of the Mn-Ga binary system. $MnGa_4$ and $MnGa_{5-x}$ display cubic and tetragonal/triclinic structures, respectively. These Ga-rich structures are characterized by the presence of "isolated" manganese atoms enclosed in gallium polyhedra. While the manganese

atoms are placed in a cubic environment of gallium in $MnGa_4$, the atomic arrangement is somewhat more complex in the Ga-richer $MnGa_{4.96}$ and $MnGa_{4.83}$. The latter crystals displaying very close stoichiometries were considered as two structural forms, correlated by a superstructure-type relationship, of the $MnGa_{5-x}$ compound. In the structure of $MnGa_{5-x}$, the manganese atoms are surrounded by gallium neighbors arranged at vertices of a capped square-antiprism. Remarkable is the absence of structural analogy with the aluminum-rich compounds in which Mn atoms are located inside coordination polyhedra whose geometries mainly derive from the isosahedron. In the gallium-rich compounds studied in this work, bonding mainly proceeds through Mn-Ga interactions, a result which validates the description of their structures in terms of Mn-centered polyhedral units. The observation of rather high electron density at interpolyhedral linking is an additional argument for such a description of $MnGa_{5-x}$ compound where some covalence locally occurs in a material predicted with a metallic behavior by DFT calculations.

Acknowledgements

FIGURE CAPTIONS

Figure 1: The reciprocal lattice projected along the 9.9Å parameter and the different unit cells mentioned in this paper. The tetragonal cell (a = 6.34, c = 10.03 Å, type B crystals) and its $3 \times 3 \times 1$ super-cell are drawn as large and small blue-filled squares, respectively. The green-filled rectangle refers to the triclinic cell (a = 6.30, b = 18.90, c = 9.94 Å, α = 90.38, β = 90.77, γ = 90.36 °, twin 1 component, type A crystals). The C-centered orthorhombic cell (a = 8.81, b = 8.95, c = 9.94 Å) and its $3 \times 3 \times 1$ super-cell given for $MnGa_6$ in reference [11] are drawn in red.

Figure 2: Schematic representation of the Ga-rich side of the Ga-Mn binary diagram.

Figure 3: The $MnGa_4$ cubic unit cell emphasizing packing of cubic $Mn@Ga_8$ units.

Figure 4: Atomic arrangement in the tetragonal $MnGa_{4.96}$ (type B) unit cell emphasizing the $Mn_2@Ga_{14}$ polyhedra (fused and capped $Mn@Ga_8$ antiprisms).

Figure 5: The tetragonal (type B) structure of $MnGa_{5-x}$: apex-sharing or interlinked $Mn_2@Ga_{14}$ units depending upon the local disorder.

Figure 6: Packing of $Mn_2@Ga_{14}$ polyhedra in the triclinic unit cell of $MnGa_{4.83}$ (type A). Excepted at center of drawing, the interpolyhedral bonding was omitted for clarity

Figure 7: Castep partial densities of states (PDOS) calculated for $MnGa_4$, tetragonal $MnGa_{5-x}$ and triclinic $MnGa_{5-x}$. The total DOS at Fermi level mainly results from gallium 4p and manganese 3d contributions.

Figure 8: The electron density difference calculated with CASTEP for $MnGa_4$ (left) and triclinic $MnGa_{5-x}$ (right). High densities, indicative of bond formation, are found at Mn-Ga atomic pairs and between the Ga atoms involved in interpolyhedral bonding in $MnGa_{5-x}$

References

[1] P. Entel, V.D. Buchelnikov, M.E. Gruner, A. Hucht, V.V. Khovailo, S.K. Nayak, A.T. Zayak, *Materials Science Forum*, 583 (**2009**) 21-41.

[2] S.W. D'Souza, J. Nayak, M. Maniraj, A. Rai, R.S. Dhaka, S.R. Barman, D.L. Schlagel, T.A. Lograsso, A. Chakrabarti, *Surface Science*, 606 (**2012**) 130-136.

[3] P. Entel, A. Dannenberg, M. Siewert, H. Herper, M. Gruner, D. Comtesse, H.-J. Elmers, M. Kallmayer, *Metallurgical and Materials Transactions A*, (**2011**) 1-10.

[4] G.D. Liu, Z.H. Liu, X.F. Dai, S.Y. Yu, J.L. Chen, G.H. Wu, *Science and Technology of Advanced Materials*, 6 (**2005**) 772-777.

[5] A. Planes, L. Manosa, M. Acet, *Journal of Physics: Condensed Matter*, 21 (**2009**) 233201.

[6] K.K. Wang, A. Chinchore, W.L. Lin, D.C. Ingram, A.R. Smith, A.J. Hauser, F.Y. Yang, *Journal of Crystal Growth*, 311 (**2009**) 2265--2268.

[7] K.K. Wang, A. Chinchore, W.L. Lin, A.R. Smith, K. Sun, *Mater. Res.Soc. Symp. Proc.*, (**2009**) 1118.

[8] M. Tanaka, J.P. Harbison, T. Sands, B. Philips, T.L. Cheeks, J. De Boeck, L.T. Florez, V.G. Keramidas, *Applied Physic Letters*, 63 (**1993**) 696.

[9] A. Grünebohm, H.C. Herper, M.E. Gruner, P. Entel, *IEEE transaction on magnetics*, 45 (**2009**) 3965-3968.

[10] H.G. Meissner, K. Schubert, T.R. Anantharaman, *Proceedings Mathematical Sciences*, 61 (**1965**) 340-367.

[11] K. Girgis, H. Schulz, *Naturwissenschaften*, 58 (**1971**) 95.

[12] T.B. Massalski, *Binary alloy phase diagrams, 2nd ed., Materials Information Soc., Materials Park, Ohio*, (**1990**).

[13] P. Villars, K. Cenzual, *Pearson's Crystal Data : crystal structure database for inorganic compounds release 2009/10, ASM international, Material Park, Ohio, USA*.

[14] O. Gourdon, G.J. Miller, *J. Solid State Chem.*, 173 (**2003**) 137-147.

[15] M. Boström, S. Hovmöller, *J. Solid State Chem.*, 153 (**2001**) 398-403.

[16] M. Boström, S. Hovmöller, *J. Alloys Compd.*, 314 (**2001**) 154-159.

[17] O.V. Dolotko, J. Pohlabeln, W. Jeitschko, *Coll. Abs. 9th Int. Conf. Crystal Chem. Intermet. Compd. (Lvov)* (**2005**).

[18] U. Haussermann, P. Viklund, M. Bostrom, R. Norrestam, S.I. Simak, *Physical Review B*, 63 (**2001**) 125118.

[19] J.S. Wu, K.H. Kuo, *Metall. Mater. Trans. A*, 28A (**1997**) 729-742.

[20] J.S. Wu, K.H. Kuo, *Micron*, 31 (**2000**) 459-467.

[21] D. Schechtmann, I. Blech, D. Gratias, J.W. Cahn, *Phys. Rev. Lett.*, 53 (**1984**) 1951.

[22] V. Petricek, M. Dusek, L. Palatinus, *Jana2006. The crystallographic computing system. Institute of Physics, Praha, Czech Republic.*, (**2006**).

[23] G.M. Sheldrick, (**1997**) SHELXS 97. A Program for Crystal Structures Solution. University of Göttingen. Germany.

[24] G.M. Sheldrick, (**1997**) SHELXL 97: A Program for Refining Crystal Structures. University of Göttingen. Germany.

[25] CrysAlis'Red' 171 software package, Oxford diffraction Ltd, Abingdon, United Kingdom. (**2004**).

[26] G. Kresse, J. Forthmuller, *J. Comput. Mater. Sci.*, 6 (**1996**) 15.

[27] G. Kresse, J. Forthmuller, *Phys. Rev.B* 54 (**1996**) 11169.

[28] J.P. Perdew, J.A. Chevary, S.H. Vosko, M.R. Pederson, D.J. Singh, C. Fiolhais, *Phys. Rev. B*, 46 (**1992**) 6671.

[29] D. Vanderbilt, *Phys. Rev. B*, 41 (**1990**) 7892-7895.

[30] H.J. Monkhorst, J.D. Pack, *Phys. Rev. B*, 16 (**1997**) 1748.

[31] I. Antonyshyn, e. al., 12th European Conference on Solid State Chemistry (ECSSC XII), Münster, September 2009.

[32] I. Antonyshyn, e. al., 18th International Conference on Solid Compounds of Transition Elements (SCTE); Lisboa, April 2012.

[33] M.J. Buerger, *Am. Mineralogist*, 30 (**1945**) 469-482.

[34] V. Hansen, J. Gjonnes, *Acta Crystallogr. A* 52 (**1996**) 125-132.

[35] P. Viklund, C. Svensson, S. Hull, S.I. Simak, P. Berastegui, U. Haussermann, *Chemistry*, 7 (**2001**) 5143-5152.

[36] U. Haussermann, M. Bostrom, P. Viklund, O. Rapp, T. Björnängen, *Journal of Solid State Chemistry*, 165 (**2002**) 94-99.

[37] *Triclinic, P1, a = 6.302, b = 9.938, c = 18.911 Å, α = 90.52, β = 90.79, γ = 90.43 ° - Monoclinic, P2,   a = 6.291, b = 9.968, c = 31.431 Å, β = 90.79 ° - Tetragonal, P4/m, a = 6.346, c = 10.023 Å*

[38] The structure of tetragonal $MnGa_{5-x}$ could be correctly refined to 4.5% in P4/m but disorder still occurs and additional glides are detected, then reverting to the symmetry P4/mnc.

[39] M. Bostrom, *Dissertation: Crystal structures and phase equilibria in the Mn-Ga system*, Stockholm, Sweden (**2002**).